Epithelial Stress and Apoptosis Underlie Hermansky-Pudlak Syndrome–associated Interstitial Pneumonia

Poornima Mahavadi[1], Martina Korfei[1], Ingrid Henneke[1], Gerhard Liebisch[2], Gerd Schmitz[2], Bernadette R. Gochuico[3], Philipp Markart[1,4], Saverio Bellusci[4], Werner Seeger[1,4], Clemens Ruppert[1,4*], and Andreas Guenther[1,4,5*]

[1]Department of Internal Medicine II, University of Giessen Lung Center, Giessen; [2]Institute of Clinical Chemistry and Laboratory Medicine, University of Regensburg, Regensburg, Germany; [3]Medical Genetics Branch, National Human Genome Research Institute, National Institutes of Health, Bethesda, Maryland; [4]Excellence Cluster "Cardiopulmonary System," University of Giessen Lung Center, Giessen; and [5]Lung Clinic Waldhof-Elgershausen, Greifenstein, Germany

Rationale: **The molecular mechanisms underlying Hermansky-Pudlak syndrome–associated interstitial pneumonia (HPSIP) are poorly understood but, as in idiopathic pulmonary fibrosis, may be linked to chronic alveolar epithelial type II cell (AECII) injury.**

Objectives: **We studied the development of fibrosis and the role of AECII injury in various murine models of HPS.**

Methods: **HPS1, HPS2, and HPS6 monomutant mice, and HPS1/2 and HPS1/6 double-mutant and genetic background mice, were killed at 3 and 9 months of age. Quantitative morphometry was undertaken in lung sections stained with hemalaun–eosin. The extent of lung fibrosis was assessed by trichrome staining and hydroxyproline measurement. Surfactant lipids were analyzed by electrospray ionization mass spectrometry. Surfactant proteins, apoptosis, and lysosomal and endoplasmic reticulum stress markers were studied by Western blotting and immunohistochemistry. Cell proliferation was measured by water-soluble tetrazolium salt-1 and bromodeoxyuridine assays.**

Measurements and Main Results: **Spontaneous and slowly progressive HPSIP was observed in HPS1/2 double mutants, but not in other HPS mutants, with subpleural onset at 3 months and full-blown fibrosis at 9 months. In these mice, extensive surfactant abnormalities were encountered in AECII and were paralleled by early lysosomal stress (cathepsin D induction), late endoplasmic reticulum stress (activating transcription factor-4 [ATF4], C/EBP homologous protein [CHOP] induction), and marked apoptosis. These findings were fully corroborated in human HPSIP. In addition, cathepsin D overexpression resulted in apoptosis of MLE-12 cells and increased proliferation of NIH 3T3 fibroblasts incubated with conditioned medium of the transfected cells.**

Conclusions: **Extensively impaired surfactant trafficking and secretion underlie lysosomal and endoplasmic reticulum stress with apoptosis of AECII in HPSIP, thereby causing the development of HPSIP.**

Keywords: pulmonary surfactant; biogenesis of lysosome-related organelle complex; adaptor protein-3; apoptosis; cathepsin D

(*Received in original form September 21, 2009; accepted in final form March 31, 2010*)

* These authors contributed equally to this article.

Supported by research grants from the European Commission through FP7 (European IPF Network [www.pulmonary-fibrosis.net] and European Lipidomics Initiative [www.lipidomics.net]), the German Research Council (Clinical Research Group 118 "Lung Fibrosis" and Excellence Cluster "Cardiopulmonary System" [www.eccps.de]), and in part by the Intramural Research Program of the National Human Genome Research Institute, National Institutes of Health, Bethesda, MD.

Correspondence and requests for reprints should be addressed to Andreas Guenther, M.D., Ph.D., Department of Internal Medicine II, University of Giessen Lung Center (UGLC), Klinikstrasse 36, 35392 Giessen, Germany. E-mail: Andreas.Guenther@uglc.de

This article has an online supplement, which is accessible from this issue's table of contents at www.atsjournals.org

Am J Respir Crit Care Med Vol 182. pp 207–219, 2010
Originally Published in Press as DOI: 10.1164/rccm.200909-1414OC on April 8, 2010
Internet address: www.atsjournals.org

AT A GLANCE COMMENTARY

Scientific Knowledge on the Subject

No reports are available to date regarding the development of pulmonary fibrosis in murine models of Hermansky-Pudlak syndrome and the underlying mechanisms of Hermansky-Pudlak syndrome–associated interstitial pneumonia in mice and humans.

What This Study Adds to the Field

Apoptosis of alveolar epithelial type II cells in Hermansky-Pudlak syndrome–associated interstitial pneumonia in both mice and humans, due to severe lysosomal and endoplasmic reticulum stress, may represent a prominent reason for development of lung fibrosis.

Hermansky-Pudlak syndrome (HPS) is a rare autosomal recessive disorder associated with oculocutaneous albinism and hemorrhagic diathesis (1). Several HPS genes have been identified in both humans and mice that encode several protein complexes, the precise function of which is only partially known and that affect various lysosome-related organelles (LROs), including the lamellar bodies of the lungs. Hence, on the basis of their role in LRO trafficking, these genes have an enormous impact on a wide range of basic physiological processes such as immune recognition, coagulation, and neuronal function (2).

Pulmonary fibrosis due to HPS, entitled Hermansky-Pudlak syndrome–associated interstitial pneumonia (HPSIP), is known to develop in patients with HPS1 and HPS4 mutations, the genes of which encode the "biogenesis of lysosome-related organelle complexes" (BLOC)-3 (2–5). HPSIP is the most serious complication and the main reason for death of patients with HPS (6–8) and usually evolves during the third or fourth decade of life. The clinical course of HPSIP shows great similarities to the disastrous fate of patients with idiopathic pulmonary fibrosis (IPF). Accordingly, the radiographic appearance of HPSIP is comparable to that of IPF and the predominant histopathological pattern is that of usual interstitial pneumonia (UIP) (9, 10).

In contrast to IPF/UIP, however, a characteristic foamy swelling of alveolar epithelial type II cells (AECII) with lamellar bodies of increased size and number ("giant lamellar body degeneration") is regularly observed in patients with HPSIP (10).

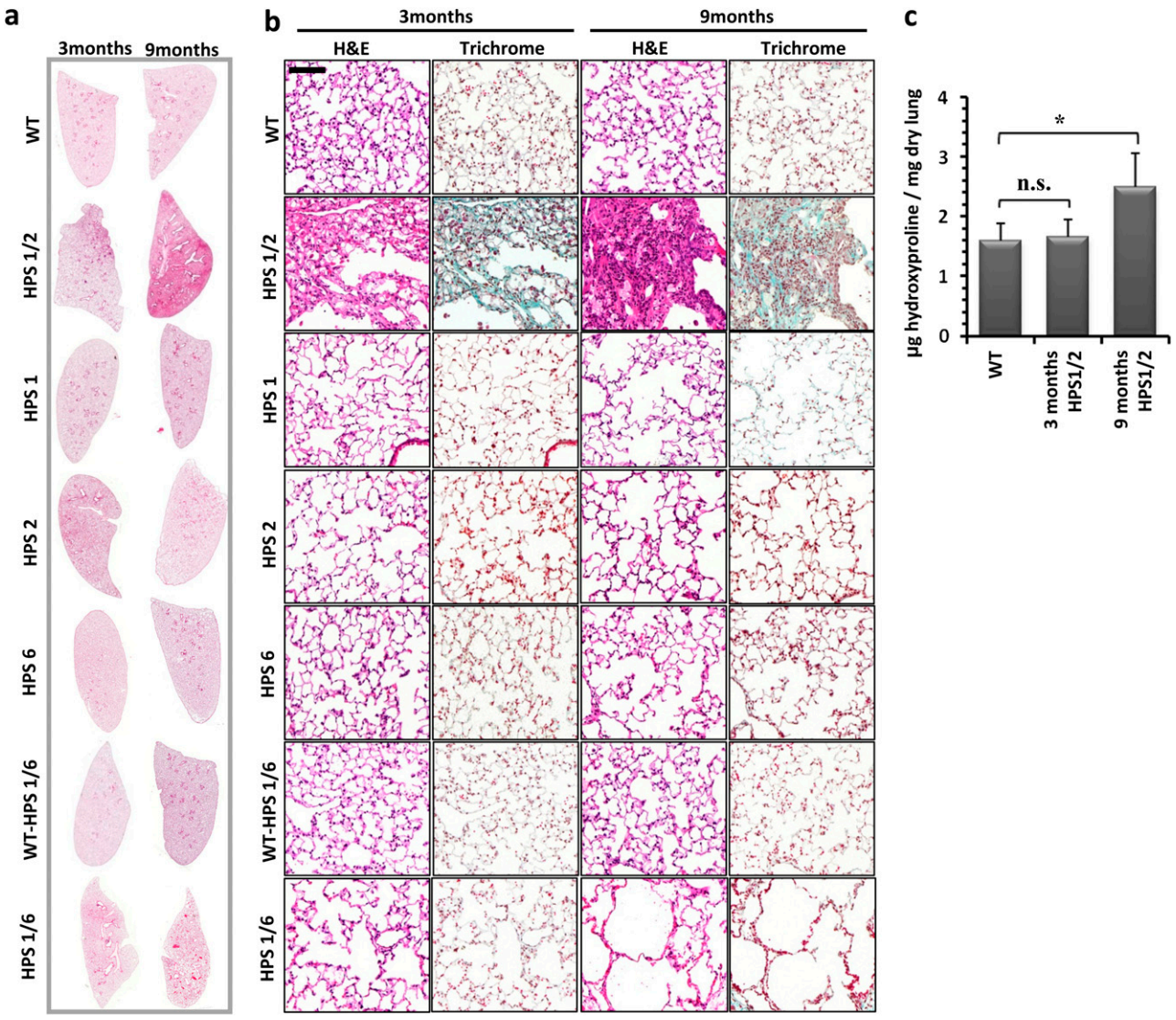

Figure 1. Development of pulmonary fibrosis only in HPS1/2 double-mutant mice: (*a*) Representative hematoxylin–eosin (H&E) stainings of complete right lungs of HPS monomutant mice, double-mutant mice, and background wild-type (WT) control mice at the ages of 3 and 9 months. (*b*) Higher magnification pictures of H&E- and trichrome-stained lungs of all the HPS mutants and WT controls analyzed in this study at the ages of 3 and 9 months. Original magnification, ×200 (scale bar, 100 μm). (*c*) Quantitative determination of lung hydroxyproline concentration in HPS1/2 double-mutant mice in comparison with WT control mice. *$P < 0.05$, n = 5 mice per group. n.s. = not significant.

As the proteins encoded by the HPS genes and their precise functions are only partly known, the pathogenesis of HPSIP is still poorly understood. However, in light of the previously mentioned histopathological findings, it has already been speculated that—like in IPF—chronic AECII injury may underlie the development of lung fibrosis (10, 11).

Interestingly, the HPS mutations occur not only in humans but also in mice, and several mono-, double-, and triple-mutant HPS mice have been characterized largely on the basis of coat color and platelet function. In some of these mice, including the herein studied HPS1/2 (*ep/pe*) mice, abnormal lung structure and abnormalities of surfactant transport and secretion in AECII had been described (12, 13). However, the development of HPSIP has not yet been described in murine HPS.

These reports prompted us to carefully assess a potential development of HPSIP in several of these murine models and to disclose potential underlying pathways. Some of the results of this study have been previously reported in the form of two abstracts (14, 15).

METHODS

Mice

Breeding pairs of HPS monomutant mice and HPS1/6 double-mutant mice were purchased from Jackson Laboratory (Bar Harbor, ME). Breeding pairs of HPS1/2 double-mutant mice were a kind gift from R. Swank (Roswell Park, Buffalo, NY). C57BL/6J was the background strain for the HPS1, HPS2, HPS6, and HPS1/2 mice. HPS1/6 mice were on the B6C3Fe background. All mice were mated and maintained under specific pathogen–free conditions, and five mice per group were killed at the ages of 3 and 9 months and genotyped as described in the online supplement.

Quantification of Lung Collagen

Hydroxyproline levels in murine lungs were determined as described elsewhere (16) and in the online supplement.

Computerized Lung Morphometry

Morphometric analysis was performed on hematoxylin and eosin–stained lung tissue sections by determining the mean interalveolar distance and mean septal thickness (linear intercept measurement). AxioVision

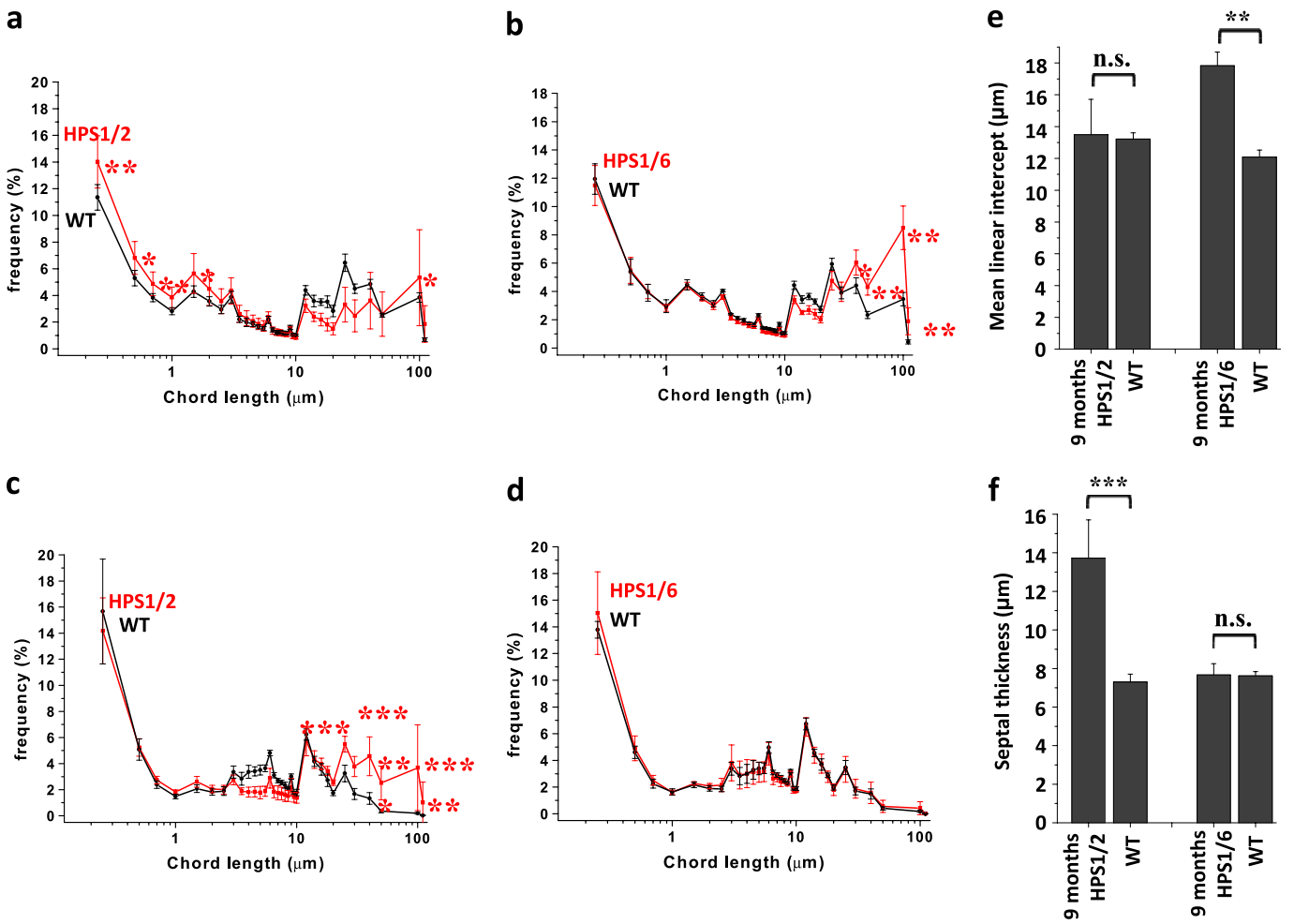

Figure 2. Increase in mean linear intercept in Hermansky-Pudlak syndrome (HPS) mice: Graphic representation of the length distribution of airspaces in (*a*) HPS1/2 mice and (*b*) HPS1/6 mice as well as the length distribution of septal thickness of (*c*) HPS1/2 mice and (*d*) HPS1/6 mice in comparison with respective wild-type (WT) controls. Twenty to 30 regions, covering the entire periphery of one digitally scanned lung slide stained with hematoxylin–eosin, were introduced with grids, comprising a total of 40,000 chords in the horizontal and vertical directions, with a distance of 40 μm. Each caption was analyzed by automated line-to-line intercept analysis, according to the criteria mentioned in METHODS. Five 9-month-old mice per group were analyzed and the data are represented as the frequency distribution of either (*a* and *b*) alveolar diameter or (*c* and *d*) septal thickness. In addition, the conventional parameters "mean linear intercept" and septal thickness are indicated in (*e*) and (*f*), respectively. ***$P < 0.001$,**$P < 0.01$, *$P < 0.05$; n.s. = not significant.

software (Carl Zeiss MicroImaging GmbH, Jena Germany) was used for the analysis as outlined in the online supplement.

Isolation of Murine Alveolar Epithelial Type II Cells

Murine AECII from the lungs of 3-month-old HPS1/2 and wild-type (WT) control mice were isolated according to the protocol given in the online supplement.

Cloning and Cell Culture

Full-length murine cathepsin D was cloned into the pcDNA3.1 expression vector and transfected into mouse lung epithelial (MLE)-12 cells, using primers and protocols described in the online supplement. NIH 3T3 mouse fibroblasts were then incubated with conditioned medium from either cathepsin D– or empty vector–transfected MLE-12 cells (24 h posttransfection). WST-1:4-[3-(4-iodophenyl)-2-(4-nitrophenyl)-2H-5-tetrazolio]-1,3-benzene disulphonate or BrdU: 5-bromo-2′-deoxyuridine (Roche Applied Science, Mannheim, Germany) was added as described in the online supplement and absorbance was measured at 450 nm.

Western Blot

Samples were subjected to denaturing sodium dodecyl sulfate–polyacrylamide gel electrophoresis followed by electroblotting on polyvinylidene difluoride membrane and immunostaining for the desired proteins. Protocol and the source of antibodies are given in the online supplement.

Phospholipid Analysis, Isolation of Large Surfactant Aggregates, and Assessment of Surface Activity

Phospholipids (PLs) were extracted from bronchoalveolar lavage fluid (BALF) or tissue extracts according to the Bligh and Dyer method as referred to in the online supplement. Characterization and surface activity of large surfactant aggregates (LAs) was undertaken as outlined in the online supplement.

Lipidomics

Lipids were quantified by electrospray ionization–tandem mass spectrometry in positive ion mode, as described in the online supplement.

Immunohistochemistry and *in Situ* Apoptosis Assay

ZytoChem Plus (AP) Broad Spectrum (Fast Red) kit (ZytoMed systems, Berlin, Germany) was used with paraffin-embedded lung sections for immunohistochemical localization of proteins according to the manufacturer's instructions. The protocol and source of antibodies are given in the online supplement. The degree of cellular

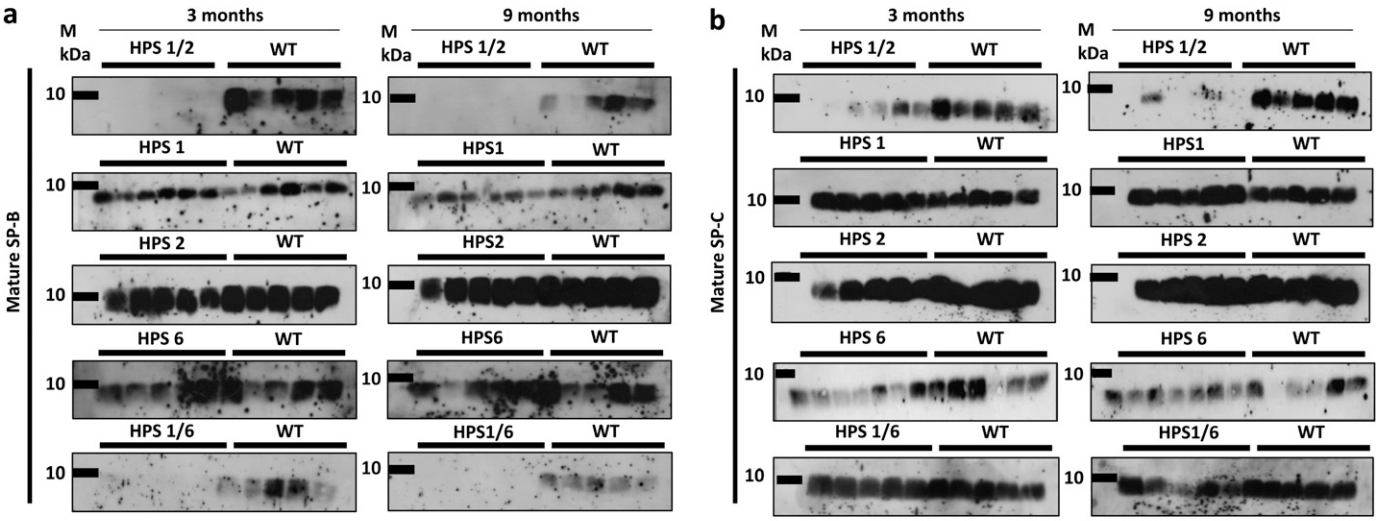

c

	Total PL content (μg/ml)	LA content (%)
WT	195.7 ± 5.86	91.3 ± 2.97
3months HPS1/2	121.5 ± 2.98 *	84.8 ± 8.13
9months HPS1/2	108.1 ± 11.18**	92.3 ± 4.81

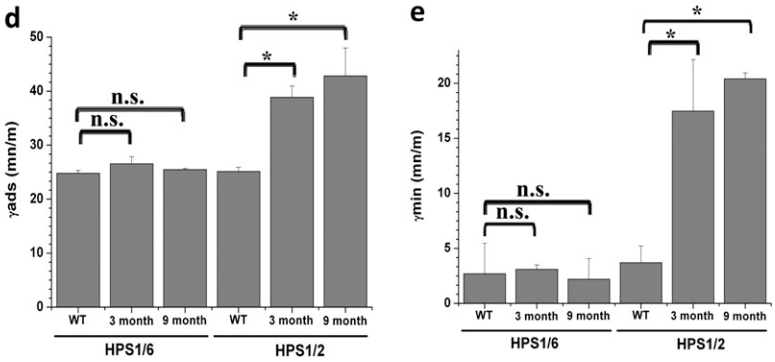

Figure 3. Loss of surfactant in bronchoalveolar lavage fluid (BALF) of HPS1/2 mice: Western blot analysis of (*a*) mature surfactant protein (SP)-B and (*b*) mature SP-C in BALF from Hermansky-Pudlak syndrome (HPS) mice along with their respective wild-type (WT) control mice at the ages of 3 and 9 months. An equal volume (20 μl per sample) of BALF was used for each analysis. (*c*) Data set showing phospholipid (PL) concentration and the relative amount of large surfactant aggregates (LA content, given as a percentage of total PL) in BALF of HPS1/2 and WT control mice. (*d* and *e*) Surface activity of LA from HPS1/2, HPS1/6, and WT control mice was characterized at a PL concentration of 2 mg/ml, employing a pulsating bubble surfactometer. (*d*) γ_{ads} (surface tension after 12 s of film adsorption) and (*e*) γ_{min} (minimal surface tension after 5 min of film oscillation) are given as millinewtons per meter (mN/m). *$P < 0.05$, **$P < 0.01$; n = 5 mice per group.

apoptosis was determined by the terminal deoxynucleotidyltransferase dUTP nick end labeling (TUNEL) method, using the *in situ* cell death detection kit, AP (Roche Applied Science) according to the manufacturer's instructions. All stained sections were analyzed on digital slide scanning, employing a Mirax scanner (Carl Zeiss GmbH, Jena, Germany). Mirax Viewer software (Carl Zeiss GmbH) was used to analyze and make snapshots of the stained tissue sections.

Statistics

Unless indicated otherwise, all data are expressed as means ± SEM of at least five mice. Statistical evaluation was performed by Mann-Whitney *U* test (comparison of two groups) and by Kruskal-Wallis *H* test (if more than two groups were analyzed). The level of significance is indicated in the figure legends and footnotes as follows: $^{*/\#}P < 0.5$, $^{**/\#\#}P < 0.01$, $^{***/\#\#\#}P < 0.001$.

RESULTS

Development of Pulmonary Fibrosis in HPS1/2

In HPS1/2 double-mutant mice, but not in HPS1/6 or HPS1, HPS2, or HPS6 mice, spontaneous development of lung fibrosis was evident at the age of 3 months (Figure 1a, *left*). Being patchy and subpleural at the beginning, the extent of lung fibrosis progressed over the age of 9 months (Figure 1a, *right*). Although fibrosis was encountered in all the 9-month-old HPS1/2 mice analyzed in this study, the extent of fibrosis differed somewhat from mouse to mouse. At higher magnification, lymphoplasmacellular infiltration and extracellular matrix deposition, with a dramatic increase in AECII size but roughly preserved lung structure, were evident at 3 months (Figure 1b). In contrast, dense fibrosis with extensive remodeling of the alveolar lung structure was prominent in 9-month-old HPS1/2 mice (Figure 1b, second row), because of which quantitative lung morphometric analysis did not reveal any significant increase in enlarged airspaces in HPS1/2 mice (Figure 2a) but revealed a more than twofold increase in septal thickness, when

TABLE 1. DIFFERENTIAL BRONCHOALVEOLAR LAVAGE COUNTS IN VARIOUS HERMANSKY-PUDLAK SYNDROME GROUPS

	AMs	PMNs	Lymphocytes
C57BL/6 controls	99.5 ± 0.7	0	0.5 ± 0.7
HPS1/2	74.6 ± 5.4	10.7 ± 6.4	14.6 ± 3.5
HPS1	67 ± 40.0	0	33 ± 40.0
HPS2	93.6 ± 10.4	0.6 ± 0.8	5.8 ± 10.4
HPS6	43.8 ± 17.9	0.4 ± 0.2	55.8 ± 23
HPS1/6 controls	99 ± 1.0	0	0.5 ± 0.7
HPS1/6	11.5 ± 4.8	0	88.5 ± 4.8

Definition of abbreviations: AMs = alveolar macrophages; HPS = Hermansky-Pudlak syndrome; PMNs = polymorphonuclear lymphocytes.
Data represent means ± SD.

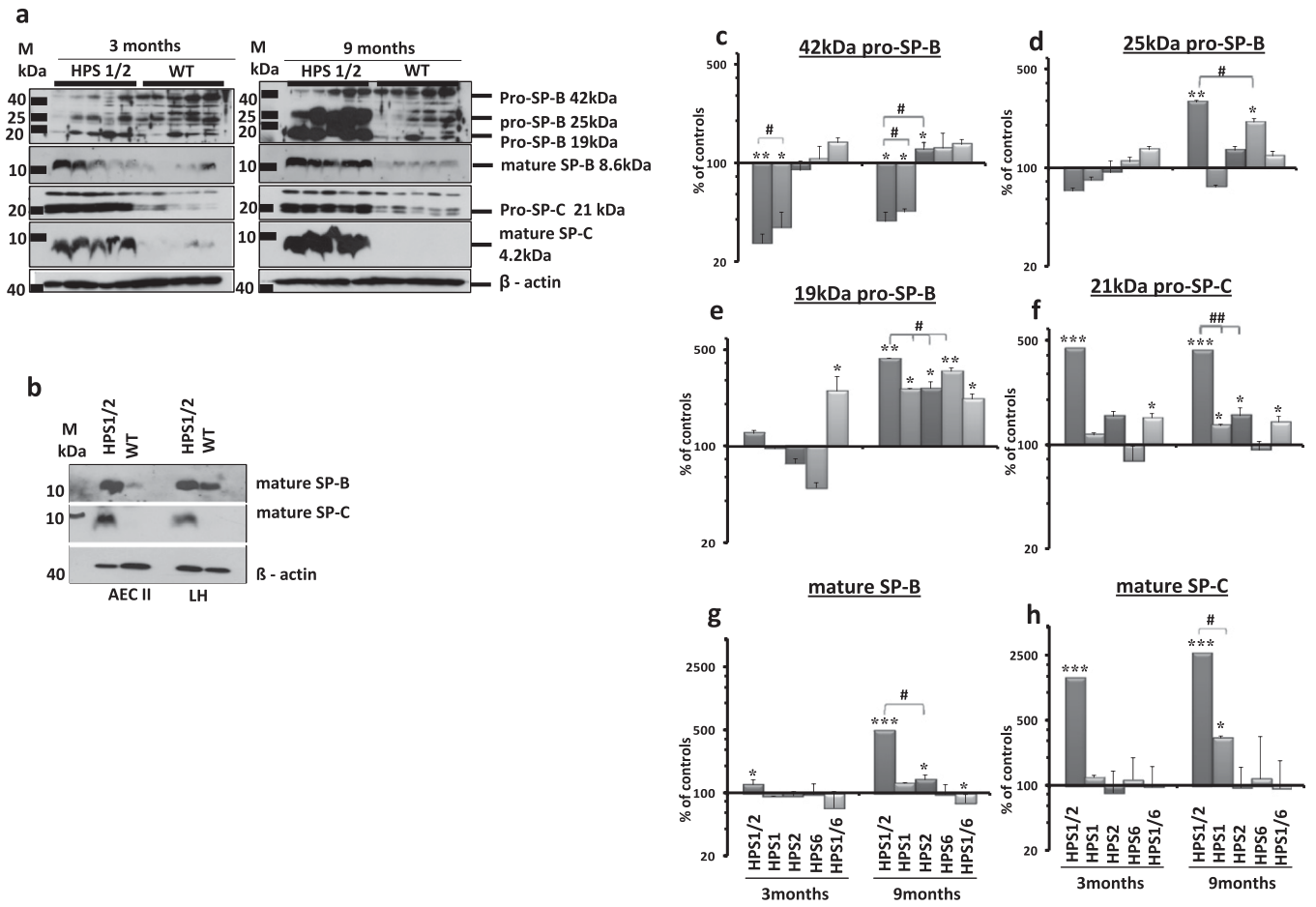

Figure 4. Accumulation of hydrophobic surfactant proteins in HPS1/2 lung tissues: (*a*) Western blot analysis of lung homogenates (LH; equal protein load) of (*left*) 3-month-old and (*right*) 9-month-old HPS1/2 double-mutant and wild-type (WT) controls for pro–surfactant protein (SP)-B, mature SP-B, pro–SP-C, and mature SP-C. (*b*) Western blot analysis of isolated alveolar epithelial type II cells (AECII; equal protein load) and LH for mature SP-B and mature SP-C from 3-month-old HPS1/2 mice and WT controls. [Please note that the blots in (*a*) and (*b*) have been developed to show adequate staining for HPS1/2 mouse samples; longer development forwarded staining for mature SP-C also in AECII and LH of WT mice.] Representative blots are from n = 5 mice per group, and three independent experiments are shown. (*c–h*) Densitometry was performed from all Western blot analyses of all HPS mouse lung homogenates. The target protein/β-actin ratio was calculated and is given as a percentage of the respective WT controls. ***$P < 0.001$,**/##$P < 0.01$, */#$P < 0.05$; n = 5 mice per group.

compared with WT controls (Figures 2c and 2e; and *see* Figure E1 in the online supplement). As a result of such fibrotic changes, lung hydroxyproline content was significantly elevated (Figure 1c). In HPS1/2 mice at 3 months, HPS1 and HPS2 monomutant mice at 9 months, and even more in HPS1/6 double-mutant mice at 9 months, airspace enlargement was a prominent finding (Figure 1b; and Figures 2b, 2d, and 2f).

Disturbed Composition and Function of the Alveolar Surfactant Pool in HPS1/2 Mice

As compared with WT mice, mature surfactant protein (SP)-B was undetectable in BALF from 3- and 9-month-old HPS1/2 mice and appeared greatly reduced in HPS1/6 mice of the same age. In contrast, BALF levels of mature SP-B remained unchanged in any of the other monomutant HPS mice (Figure 3a). Similarly, significantly reduced levels of mature SP-C were observed in the BALF of HPS1/2 mice at 3 and 9 months, but appeared unchanged in all other HPS mutants (Figure 3b). In addition, the total phospholipid content, but not the relative content of large surfactant aggregates (LAs), was significantly decreased in BALF from HPS1/2 mice (Figure 3c). As compared with WT controls, LA preparations from HPS1/2 BALF, but not from HPS1/6 BALF, showed a significant reduction in surface activity (Figures 3d and 3e). From these data, we concluded that HPS1/2 mice do have a significant defect in surfactant secretion, resulting in inappropriately low alveolar phospholipid and surfactant protein concentrations, thus leading to increased alveolar surface tension.

In addition, BALF cellular profiles from various HPS mice were analyzed. Of interest, many enlarged alveolar macrophages were encountered (data not shown), especially in HPS1/2 mice. In addition, a modest lymphocytic alveolitis was observed in all of the HPS mice analyzed (Table 1), and there was no significant difference between HPS1/2 and the other mice.

Accumulation of Hydrophobic Surfactant Proteins in HPS1/2 Lungs

A dramatic increase in intracellular content of almost all forms of the pro- and mature forms of the hydrophobic surfactant proteins SP-B and SP-C was encountered in lungs of HPS1/2 mice in comparison with their respective WT controls (Figure 4a). At the age of 3 months, especially 21-kD pro–SP-C, mature SP-B, and mature SP-C were elevated. In 9-month-old HPS1/2 mice, a more extensive accumulation of all pro- and mature

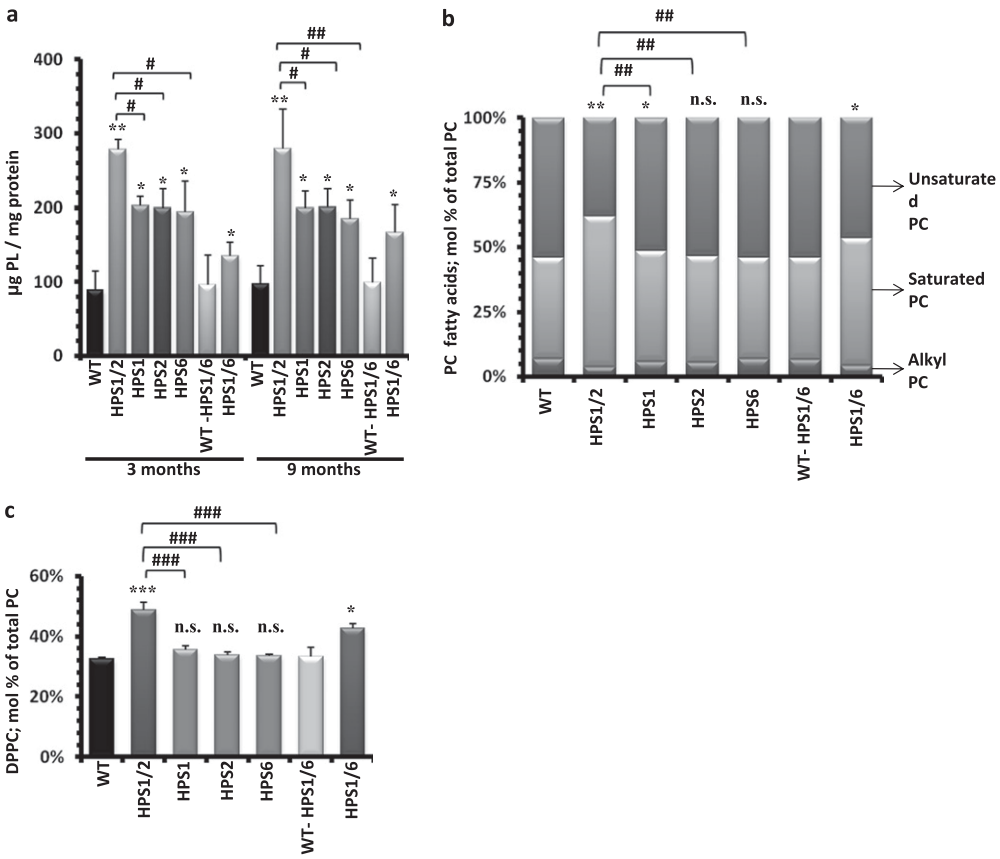

Figure 5. Accumulation of surfactant phospholipids in HPS1/2 mouse lungs: (*a*) Total phospholipids were extracted from lung tissue of all 3- and 9-month-old Hermansky-Pudlak syndrome (HPS) and wild-type (WT) control mice. The resulting phospholipid (PL) concentrations were normalized against their respective protein concentrations and values are expressed as micrograms of phospholipids per milligram of protein. (*b* and *c*) Lipidomic study was performed for 9-month-old HPS mice as compared with the respective WT control mice. *Columns* depicted here represent fatty acid distribution of (*b*) the phosphatidylcholine (PC) fraction and (*c*) the relative content of dipalmitoylated phosphatidylcholine (DPPC) within the PC fraction. Values are expressed as the molar percentage (mol %) of the respective lipid class, related to total PC. $^{*/\#}P < 0.05$, $^{**/\#\#}P < 0.01$, $^{***/\#\#\#}P < 0.001$; n.s. = not significant; n = 5 mice per group.

forms of SP-B/C, with the exception of 42-kD pro–SP-B, was encountered (Figure 4a). Densitometric analysis revealed a 25-fold increase in mature SP-C and a 5-fold increase in mature SP-B in HPS1/2 lung homogenates (Figures 4g and 4h). To confirm that such accumulation would reflect the situation within the AECII, the intracellular SP-B/C content was analyzed in AECII isolated from 3-month-old HPS1/2 mice and WT mice. Accumulation of mature SP-B and SP-C was seen exclusively in the AECII of HPS1/2 mice (Figure 4b), but not in any other HPS mutants (Figure E2). Regarding the proforms, only 19-kD pro–SP-B appeared highly up-regulated in all HPS mice (although significantly higher in HPS1/2), and some minor increases were encountered for 21-kD pro–SP-C and 25-kD pro–SP-B in these mice (Figures 4c−4f; and *see* Figure E2). Gene expression analysis did not show any differences in the expression of SP-B and SP-C between HPS1/2 and control mice (Figure E3a). Consistent with previous reports on the subcellular distribution of pro- and mature forms of the hydrophobic surfactant proteins in healthy AECII (17, 18) and with the ultrastructural appearance of AECII in humans with HPSIP (10), mature surfactant compounds seem to accumulate in the distal part of the lysosomal transport axis of AECII from HPS1/2, and hence largely in lamellar bodies.

Accumulation of Surfactant Phospholipids in HPS1/2 Lungs

We next analyzed the total phospholipid content of lung homogenates in all HPS mono- and double-mutant mice along with their WT controls. Phospholipid content was increased in all HPS mice, but to various extents. The strongest increase was found in HPS1/2 mice (approximately threefold), which was also significantly higher as compared with all other HPS mice (Figure 5a). It seems noteworthy to mention that, in contrast to the changes in mature SP-B/C, the phospholipid content of HPS1/2 lung homogenates did not further increase beyond the age of 3 months. In AECII, the combinatory loss of HPS1 and HPS2 genes thus does not seem to affect early lysosomal transport processes, as suggested for HPS1 or HPS2 gene products in other cell types (19, 20).

Lipidomic Profiling in HPS Mice

Because we observed differences in total phospholipids in HPS mice, we further performed mass spectrometry–based lipidomics analysis of lung tissues from all 9-month-old HPS and WT control mice. As evident from Table E1 in the online supplement and Figure 5a, extensive alterations of the phospholipid profile were encountered. In particular, HPS1/2 mice showed a significant increase in phosphatidylcholine (PC). To some extent this also held true for HPS1/6 mice. Of note, phosphatidylethanolamine plasmalogens were markedly depressed in HPS1/2 versus the other mice (Table E1). Moreover, a significant increase in saturated PC species was encountered in HPS1/2 mice and, to some extent, also in HPS1/6 mice (Figure 5b), which could be ascribed almost entirely to a marked increase in dipalmitoylated phosphatidylcholine (DPPC, PC-32:0; Figure 5c). Another interesting observation was a significant increase in glucosylceramides (GlcCer) in 9-month-old HPS1/2 mice, with a ceramide/GlcCer ratio of 3.9 in HPS1/2 mice compared with 7.6 in controls (*see also* Table E2). Because the expression level of the synthesizing enzyme (glucosylceramide synthase) remained unchanged (data not shown), the observed accumulation of GlcCer in HPS1/2 mice might be due to their decreased clearance.

AECII Apoptosis in HPS1/2 Mice

Accumulation and impaired secretion of pulmonary surfactant may have resulted in chronic cell stress and apoptosis of AECII

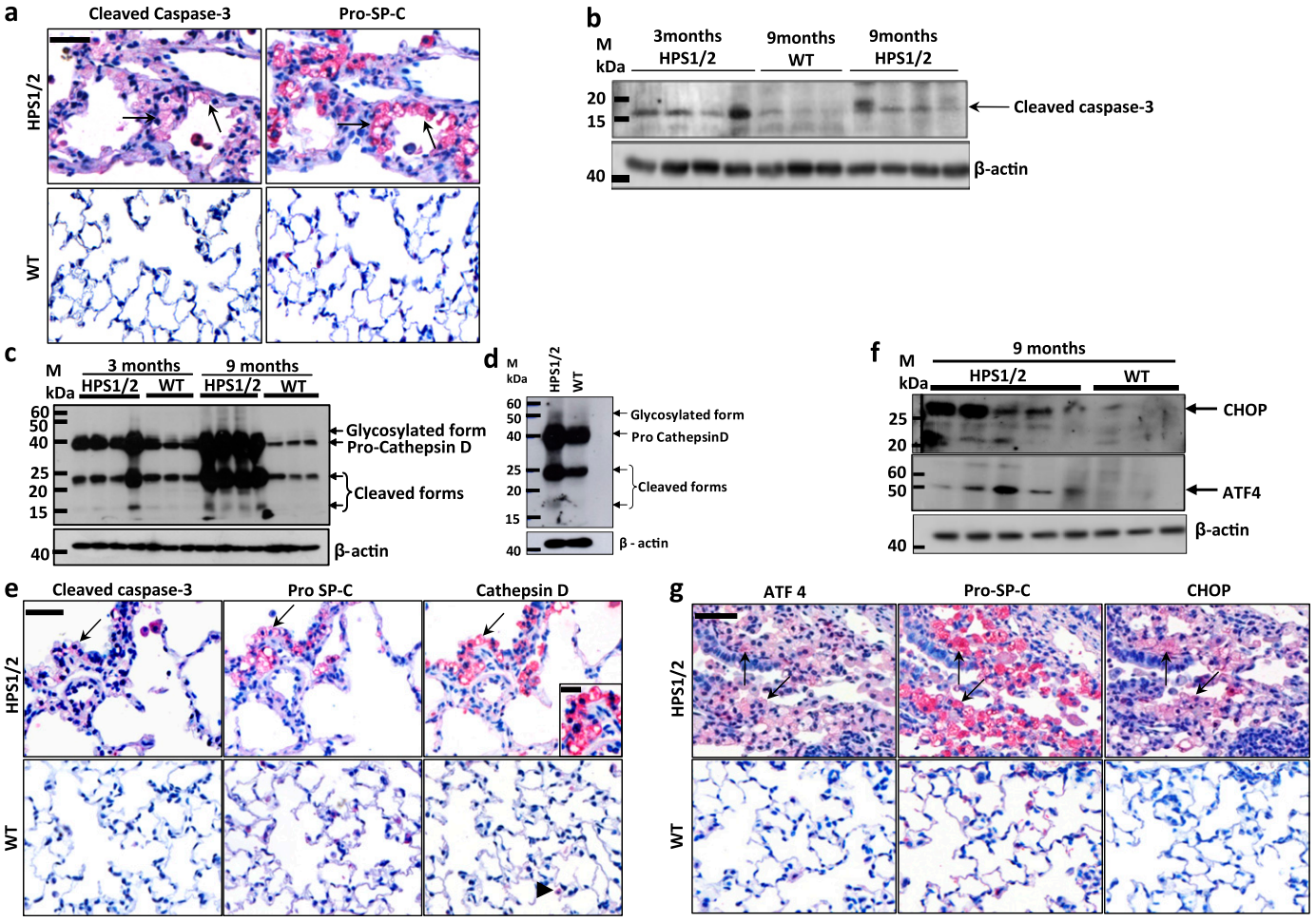

Figure 6. Alveolar epithelial type II cell (AECII) stress and apoptosis in HPS1/2 mice: (*a*) Serial paraffin-embedded lung tissue sections from (*top*) 9-month-old HPS1/2 mice and (*bottom*) wild-type (WT) controls were immunostained either for (*left*) cleaved caspase-3 or (*right*) pro–surfactant protein (SP)-C. *Arrows* indicate the same AECII stained for both proteins. (*b*) Western blot analysis of cleaved caspase-3 in lung homogenates of 3- and 9-month-old HPS1/2 mice in comparison with that of 9-month-old WT controls. (*c* and *d*) Western blot analysis of cathepsin D in (*c*) lung homogenates of HPS1/2 mice (3 and 9 mo of age) and in (*d*) isolated AECII of HPS1/2 and WT controls (3 mo of age). (*e*) Immunohistochemistry on serial sections of (*top*) HPS1/2 and (*bottom*) WT mouse lungs for (*left*) cleaved caspase-3, (*middle*) pro–SP-C, and (*right*) cathepsin D. *Arrows* indicate positive staining of AECII for all three proteins. *Inset*: High-magnification image, illustrating diffuse cytoplasmic staining of cathepsin D within the AECII of HPS1/2 mice. *Arrowhead* indicates cathepsin D staining in macrophages in a WT mouse lung tissue section. (*f*) Western blot analysis for activating transcription factor-4 (ATF4) and C/EBP homologous protein (CHOP) in lung homogenates of HPS1/2 mice and age-matched WT controls. (*g*) Serial sections were stained for either (*left*) ATF4, (*middle*) pro–SP-C, or (*right*) CHOP in 9-month-old HPS1/2 and WT controls. *Arrows* indicate the same AECII stained positive for all three proteins. Original magnification, ×400 (*scale bar*, 50 μm). Original magnification of *inset*, ×800 (*scale bar*, 20 μm). Representative blots and stainings from each group are shown, from n = 5 mice per group.

in lungs of HPS1/2 mice. To identify apoptotic AECII, we performed immunohistochemistry for cleaved, activated caspase-3, along with pro–SP-C on serial sections of HPS1/2 and control mouse lungs. It was found that the pro–SP-C–positive cells (AECII) also stained positive for cleaved caspase-3 in HPS1/2 tissue sections, whereas no signal for cleaved caspase-3 was detected in any WT control (Figure 6a). Western blot analysis for caspase-3 produced a similar result (Figure 6b). Alternatively, we performed TUNEL staining, along with immunohistochemistry, for the AECII-specific marker pro–SP-C on serial sections from all HPS and control mice. As depicted in Figure E4a in the online supplement, numerous TUNEL-positive AECII were already evident only in the lung tissue of HPS1/2 mice at an age of 3 months (but not in other mutants), indicating that AECII apoptosis is an early event in these mice. Thus, TUNEL data fully confirmed the cleaved caspase-3 immunohistochemistry and again suggest that AECII undergo extensive apoptosis in HPS1/2 mice, but not in other HPS or control mice.

Lysosomal and Endoplasmic Reticulum Stress Underlie AECII Apoptosis in HPS1/2 Mice

Observations to this point indicated that intracellular accumulation of surfactant was especially prominent in HPS1/2 mice and possibly related to the increased apoptosis of AECII, thus favoring fibrosis development in HPS1/2 double-mutants. To further study the pathways that may interconnect surfactant accumulation and AECII apoptosis in HPS1/2 mice, it was hypothesized that such surfactant accumulation may cause primarily lysosomal stress in these mice. Therefore, a well-known lysosomal aspartyl protease, cathepsin D, which has been shown to induce apoptosis by several mechanisms (21, 22), was analyzed by Western blotting. Increased levels of procathepsin D (~44 kD), its glycosylated form (~54 kD), and

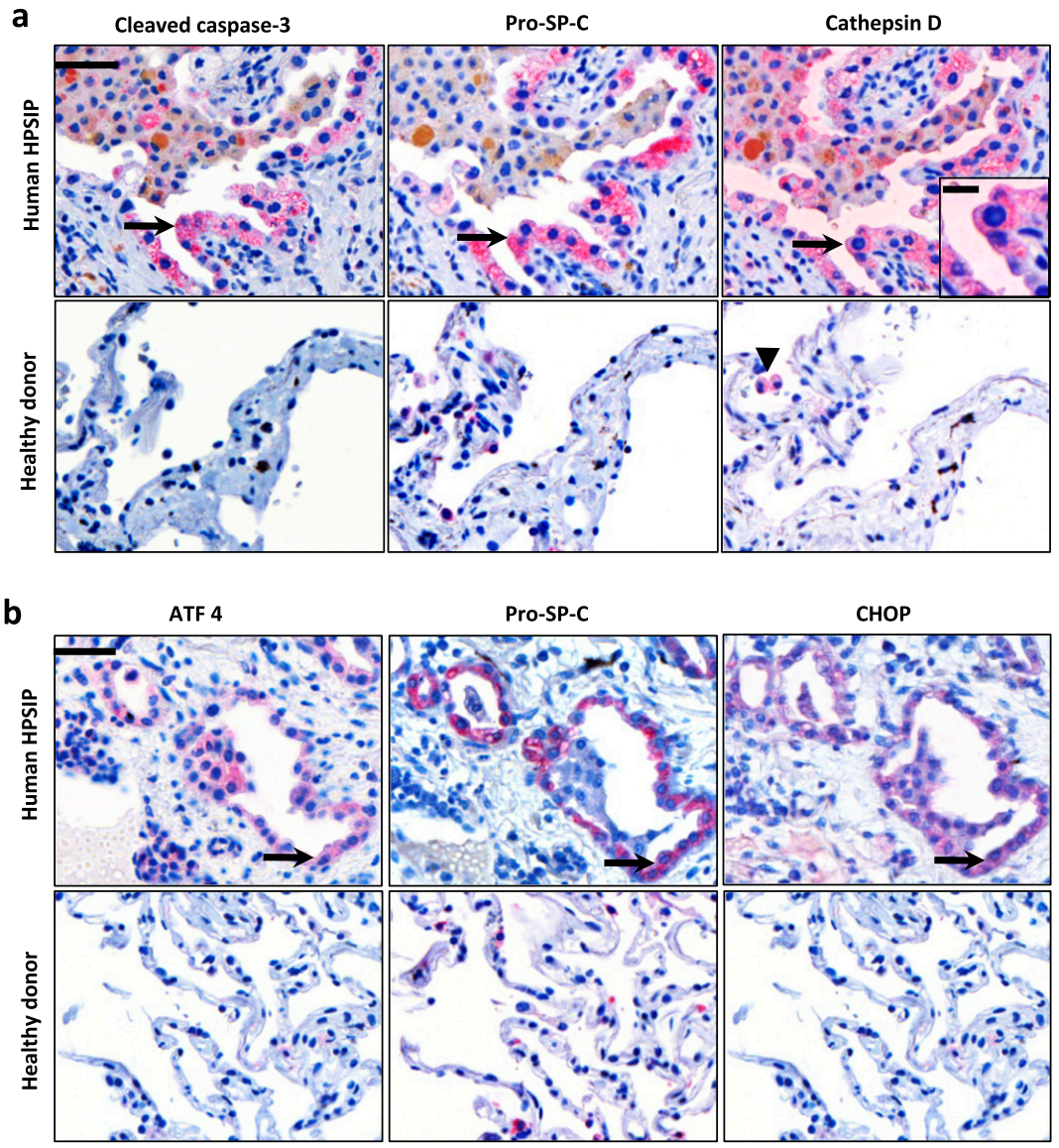

Figure 7. Apoptosis of alveolar epithelial type II cells (AECII) due to lysosomal and endoplasmic reticulum stress in human Hermansky-Pudlak syndrome–associated interstitial pneumonia (HPSIP): (*a*) Representative immunohistochemistry performed on serial paraffin-embedded lung tissue sections from (*top*) human patients with HPS and (*bottom*) healthy donors for (*left*) cleaved caspase-3, (*middle*) pro–surfactant protein (SP)-C, and (*right*) cathepsin D. *Arrows* indicate the same AECII stained for all three proteins. *Inset*: High-magnification image, illustrating diffuse cytoplasmic staining of cathepsin D within the AECII of HPSIP. *Arrowhead* indicates cathepsin D staining in macrophages in a lung tissue section of a healthy donor. (*b*) Serial lung tissue sections from (*top*) human patients with HPS and (*bottom*) healthy donors were stained for (*left*) activating transcription factor-4 (ATF4), (*middle*) pro–SP-C, or (*right*) C/EBP homologous protein (CHOP). *Arrows* indicate positive staining of an AECII for all three proteins. Representative sections from patients with HPS1 and four healthy donors are shown. Original magnification, ×400 (*scale bar*, 50 μm). Original magnification of *inset*, ×800 (scale bar, 20 μm).

subsequent cleavage products were observed in lung homogenates of 3- and 9-month-old HPS1/2 mice and in the AECII of 3-month-old HPS1/2 mice when compared with respective controls (Figures 6c and 6d). Interestingly, cathepsin D levels in lung homogenates of all other HPS mice were found to be virtually identical (*see* Figures E5a–E5c in the online supplement). Cathepsin D gene expression in HPS1/2 mice, however, did not differ from controls (Figure E5d). In colocalization studies employing immunohistochemistry for cathepsin D, cleaved caspase-3, and pro–SP-C on serial sections, we identified all three proteins on identical regions in HPS1/2 lungs (Figure 6e) with a pan-cytoplasmic distribution pattern for cathepsin D (inset in Figure 6e).

Apart from the lysosomal stress response, the possible existence of an endoplasmic reticulum (ER) stress response was also assessed in HPS mice. For this purpose, the late ER stress marker C/EBP homologous protein (CHOP; GADD153), which represents an obligatory and important proapoptotic ER stress compound, as well as activating transcription factor-4 (ATF4), which serves as a direct transcription factor for CHOP, were studied. Western blot analysis using lung homogenates revealed an up-regulation of both proteins in HPS1/2 mice, at the age of 9 months (Figure 6f) but not at an age of 3 months (data not shown). To check whether the ATF4 and CHOP signals of lung homogenates originate from AECII, immunohistochemistry of ATF4, CHOP, and pro–SP-C was performed on serial sections. Interestingly, these stainings illustrated that pro–SP-C–positive cells stained positive for ATF4 and CHOP in lung sections from 9-month-old HPS1/2 mice, whereas control mouse sections showed no positivity (Figure 6g), thus indicating that AECII from HPS1/2 mice undergo ER stress during a later stage of the disease.

AECII Apoptosis Due to Lysosomal and ER Stress Is Also a Prominent Finding in Human HPSIP

Lysosomal and ER stress pathways were characterized in human HPSIP. Lack of frozen lung material from transplanted human patients with HPS restricted the current work to available serial lung sections from paraffin-embedded lung tissues from only two patients with HPS, on which immunohistochemistry was performed. Interestingly, AECII from patients with HPSIP not only showed much more pronounced reactivity for pro–SP-C as compared with donor lungs, but also showed positive staining for both cleaved caspase-3 and cathepsin D

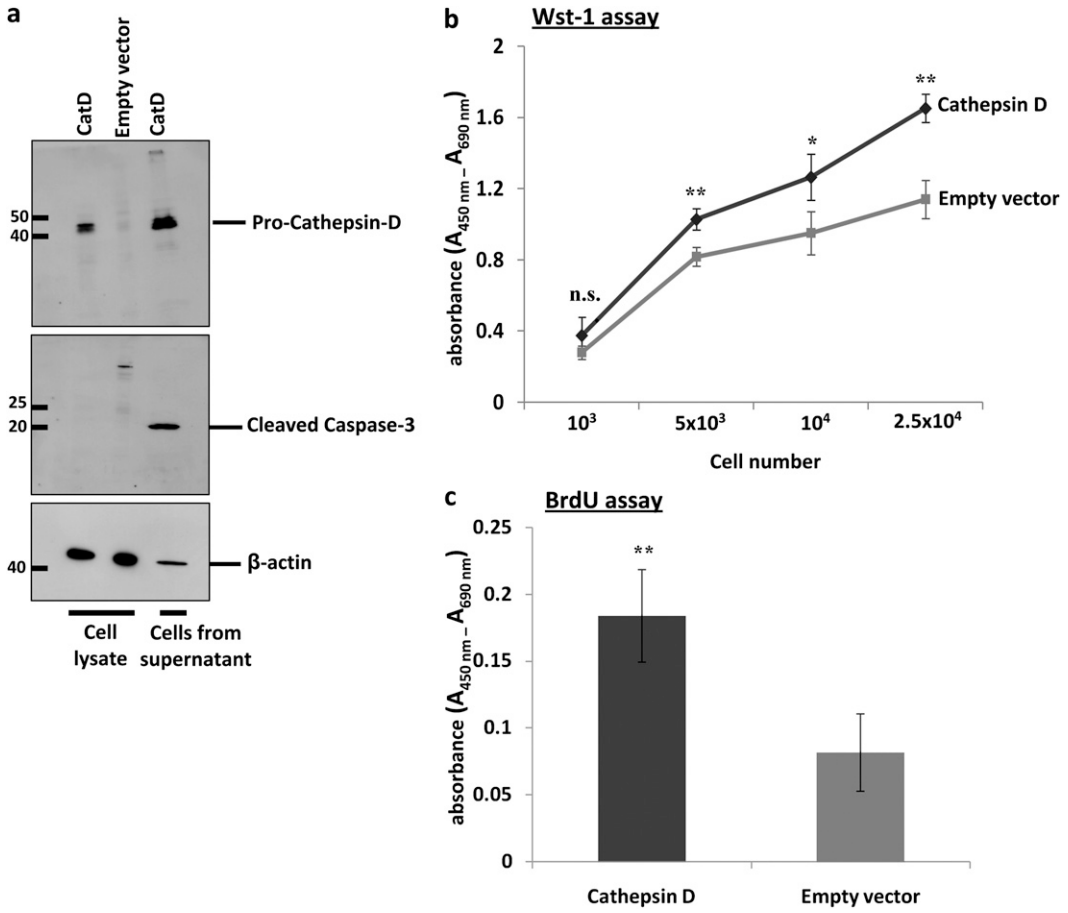

Figure 8. Overexpression of cathepsin D (CatD) drives apoptosis of an alveolar epithelial cell line and proliferation of fibroblasts: (*a*) Total protein extracts prepared from cathepsin D– and empty vector–transfected mouse lung epithelial (MLE)-12 cells as well as cells collected from supernatant after cathepsin D transfection (after 24 h) were subjected to Western blotting for (*top*) cathepsin D and for (*middle*) cleaved caspase-3, with equal protein loading (β-actin, *bottom*). Supernatant from cells transfected with empty vector did not contain enough cells (protein) to be included. (*b* and *c*) Conditioned medium from either cathepsin D– or empty vector–transfected MLE-12 cells was applied to an equal number of NIH 3T3 fibroblasts and their viability was assessed by (*b*) water-soluble tetrazolium salt (WST)-1 assay at various cell numbers or their proliferation was measured by (*c*) bromodeoxyuridine (BrdU) incorporation. $*P < 0.05$, $**P < 0.01$; n.s. = not significant.

(Figure 7a), thus fully confirming the data observed in the elder and fibrotic HPS1/2 mice. Diffuse cytoplasmic staining for cathepsin D within AECII was also observed in lung sections of HPSIP (inset in Figure 7a). Of interest, in healthy lung tissues from mice (Figure 6e) and humans (Figure 7a) cathepsin D staining was observed primarily in alveolar macrophages but not in AECII, again underscoring the significance of the observed increase in cathepsin D in AECII under conditions of HPSIP. In addition, we investigated the expression of the proapoptotic ER stress factor CHOP and its transcription factor ATF4 in human HPSIP. As depicted in Figure 7b, immunoreactivity for CHOP and ATF4 was found in AECII of HPSIP lungs, but not of donor lungs, again providing evidence for a proapoptotic ER stress response in the AECII of these patients.

Cathepsin D Promotes Apoptosis of Alveolar Epithelial Cell Line and Fibroblast Proliferation

In addition, to assess the causative role of cathepsin D overexpression in alveolar epithelial cell apoptosis and its role in fibroblast proliferation, we overexpressed full-length mouse cathepsin D in AECII-like MLE-12 cells. By analysis of cleaved caspase-3, we observed significant cell death in cathepsin D–transfected cells, as compared with empty vector–transfected cells (Figure 8a). These cells were largely detached from the culture plate, 24 hours posttransfection. Conditioned medium from cathepsin D–transfected cells was then applied on NIH 3T3 fibroblasts and this resulted in increased viability and proliferation, as measured by WST-1 assay (Figure 8b) and BrdU incorporation (Figure 8c), respectively. Incubation of NIH 3T3 fibroblasts with conditioned medium from empty vector–transfected cells resulted in a significantly depressed proliferative signal.

DISCUSSION

In patients with HPS, impaired lysosomal trafficking axis causes a complex spectrum of cell- and organ-specific disturbances, including severe pulmonary fibrosis in a larger subpopulation of patients with HPS1 and HPS4 mutations. Another entity caused by disturbed lysosomal transport is the Chédiak-Higashi syndrome (CHS), a bleeding disorder with severe and recurrent infections. In murine models of CHS (beige mice with a mutation in lysosomal trafficking regulator lyst1 [23], and chocolate mice with a rab38 mutation [24]), increased cellularity and modest interstitial inflammation have been described (23, 24), and emphysema was a prominent finding in HPS1/2 (12). In chocolate mice and in HPS1/2 mice, accumulation of mature surfactant components and giant lamellar body degeneration have been described to various extents. However, this is the first study to show spontaneous development of lung fibrosis in a murine model of HPS, which fully mimicks clinical HPSIP.

An obvious explanation for phenotypic differences in different mouse models may be that, as compared with HPS1/2, in other models, the accumulation of intracellular surfactant levels may not have reached a critical threshold level to induce chronic cellular stress and AECII apoptosis. In line with this, beige mice exhibit modest PC (~1.5-fold) and SP-B accumulation in lung homogenates, a slight reduction of SP-B in BALF at 24 weeks, and only a twofold increase in disaturated PC in adulthood (25). Regarding the surfactant pool size in tissue and

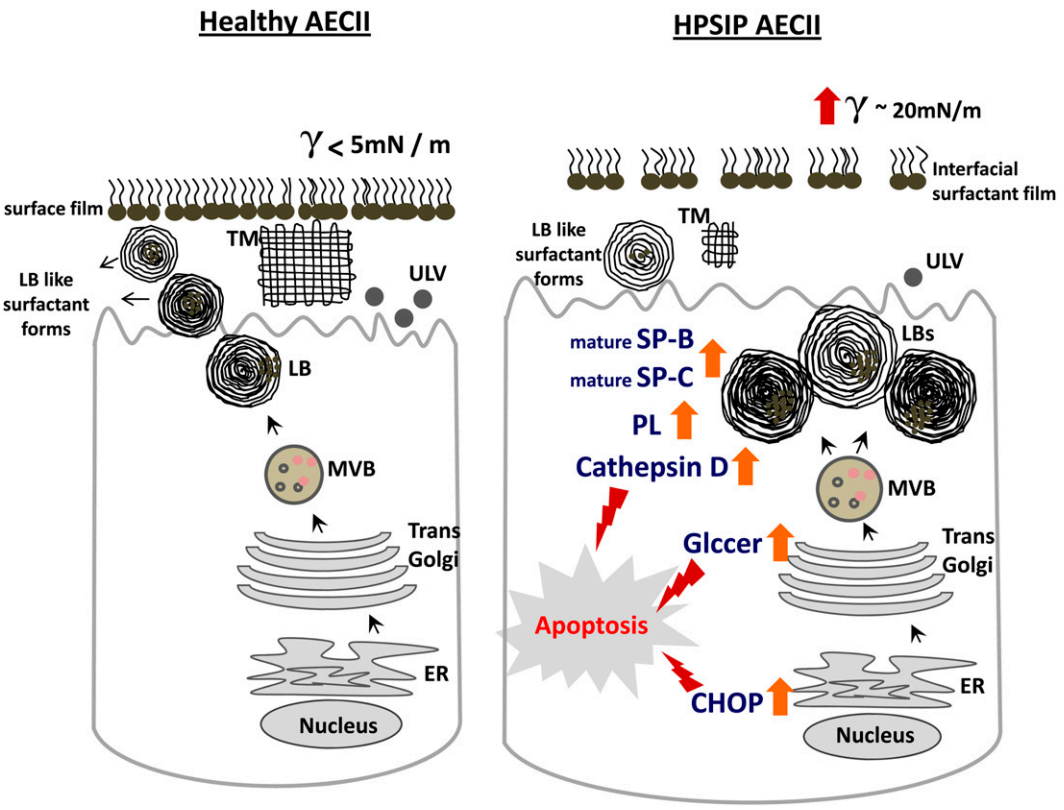

Figure 9. Proposed model for induction of apoptosis of alveolar epithelial cells type II (AECII) in Hermansky-Pudlak syndrome–associated interstitial pneumonia (HPSIP) lungs: On the *left*, a healthy AECII is shown, with regular surfactant processing, transport, and secretion. On the *right*, our data on HPSIP are summarized, in which giant lamellar bodies, defective surfactant transport, and impaired secretion of surfactant are shown. Alveolar surface tension in HPSIP lungs is increased, indicating the reduced surface activity of the alveolar surfactant pool in these lungs. Within the AECII, an increase in cathepsin D, glucosylceramides, and CHOP-induced apoptosis of the cell may result in the development of lung fibrosis. CHOP = C/EBP homologous protein; ER = endoplasmic reticulum; Glccer = glucosylceramides; LBs = lamellar bodies; MVB = multivesicular bodies; PL = phospholipids; SP = surfactant protein; TM = tubular myelin; ULV = unilamellar vesicles.

airspace enlargement, these mice are thus comparable to HPS1, HPS2, HPS6, and HPS1/6 mice (26), but they do not seem to develop fibrosis. Several factors may contribute to the development of lung fibrosis exclusively in HPS1/2.

First, activation of macrophages and elevation of basal inflammatory cytokine levels, as reported for HPS1 and HPS2 mice (23, 27), may also support fibrotic reactions. Indeed, macrophage activation has also been described in patients with HPS1 mutations (28). On the other hand, with the exception of altered morphology of macrophages (data not shown), our HPS1/2 mice did not show a significantly different differential cell count as compared with the other genotypes. Although such assessment is certainly incomplete, it does not suggest a substantially different level of inflammatory changes between mice that develop fibrosis and those that do not.

Second, changes in the extracellular surfactant pool may contribute to the development of lung fibrosis. In HPS1/2 mice, we now observed greatly increased alveolar surface tension paralleled by a far-reaching absence of both hydrophobic surfactant proteins, most likely reflecting the severity of the intracellular transport deficiency. In contrast, although also almost deficient in SP-B at the alveolar level, HPS1/6 mice still had reasonably high amounts of SP-C in the alveolar space and, accordingly, normal surface tension–reducing characteristics of the alveolar surfactant film. At a quick glance, such an observation may place SP-C at the center of a pathomechanistic concept, especially bearing in mind that SP-C may well play a role in maintaining lung mechanics (as suggested with SP-C$^{-/-}$ mice [29]). However, we believe that the loss of surface activity in HPS1/2 mice is more simply related to the simultaneous loss of SP-B and SP-C at the alveolar level, a feature well known from term babies with respiratory distress, in whom a complete (no gene expression) loss of SP-B and a functional (no processing of pro–SP-C) loss of SP-C are encountered (30). At present, we certainly cannot exclude a pathomechanistic role of the increased alveolar surface tension in the process of lung fibrosis, especially when keeping in mind the role of biomechanical forces in fibroblast activation (31). Further experiments are needed to precisely define the role of elevated alveolar surface tension, a common feature in, for example, subjects with IPF (32), in the development of lung fibrosis.

Third and, from our understanding, most importantly, an intriguing interpretation of our data and those of others is that the observed accumulation of mature and intermediate surfactant compounds in AECII may be of potential harm for this cell type and that—depending on the cellular stress level—airspace enlargement or lung fibrosis may represent the phenotypic consequences. Such an idea is supported by our observation that conditioned medium from cathepsin D–transfected epithelial cells, which are prone to apoptosis, promotes fibroblast proliferation.

In contrast to mice, in which HPSIP is provoked only by a double hit affecting both HPS1 and HPS2 (33), single mutation of HPS1 or HPS4 in humans resulted in HPSIP (4, 34, 35). In higher eukaryotes, HPS1 and HPS4 encode BLOC (biogenesis of lysosomal-related organelle complex)-3 (36), which was suggested to regulate endosomal and lysosomal movements by microtubule- and actin-dependent mechanisms (37–39). Adaptor protein (AP)-3 is affected in HPS2 and has been suggested to play a role in transporting selected proteins from *trans*-Golgi to lysosomes, endosomes, or lysosome-related organelles and was shown to form a tripartite complex with BLOC-1 and phosphatidylinositol-4-kinase type II α (PI4KIIa) (40). Interestingly, one study showed anatomically different AP-3–regulatory mechanisms in brain (41). It is also known to directly interact with some other HPS gene products (but never with BLOC-3) and cellular factors involved in lysosomal trans-

port and secretion (42, 43). Similarly, in samples from patients with HPS1 mutations, the intracellular localization of the AP-3 complex remained unaltered in fibroblasts (44, 45). Drawn against this background and observations by Feng and colleagues (46), it appears highly unlikely that AP-3 directly interacts with HPS1/BLOC-3, although these studies have never been performed in active secretory cells in general and in AECII in particular. Of note, in HPS1/2 mice, cumulative accumulation of lysosomal enzymes (β-glucuronidase, β-galactosidase) in lungs and kidneys again supports the concept of a functional redundancy of HPS1 and HPS2 in surfactant trafficking (46). Hence, only if both complexes are affected in parallel will extensive accumulation of surfactant, cell stress, and apoptosis occur, leading to fibrosis in mice (Figure 9). Although unclear at present, a lack of functional redundancy between BLOC-3 and AP-3 in humans could be a potential explanation for the development of HPSIP with single BLOC-3 or AP-3 mutations.

Another explanation for all these differences between mice and humans could involve environmental (e.g., smoking) or medical factors. Regarding the latter, steroids and β-mimetics, agents that may be frequently used in subjects with HPSIP, may in fact increase surfactant expression and production and aggravate the level of intracellular stress (47).

In general, HPS proteins were suggested to be responsible for (*1*) cargo sorting and transport vesicle formation, (*2*) movement of transport carriers across the cytoskeletal axis, and (*3*) tethering, docking, and fusion of vesicles at the target membrane (48). In view of the herein described accumulation of mature surfactant compounds in HPS1/2, it appears likely that the biosynthetic surfactant pathway is affected more in the distal part, starting at the level of the multivesicular body (MVB; Figure 9), as it is well known that the MVB is the earliest lysosomal organelle in which maturation of SP-B/C occurs. The inability of isolated AECII from HPS1/2 mice to adequately secrete surfactant even in response to ATP (13) lends credence to the assumption that a more distal transport process is altered in HPS1/2 mice.

Consistent with such reasoning, we observed an early lysosomal stress reaction in HPS1/2 mice, characterized by a significant increase in cathepsin D levels in AECII. Although representing a normal lysosomal constituent, cathepsin D potentially induces apoptosis in many cell types (21, 22) via different mechanisms (49–51). Supporting this view, in the present study, we observed apoptosis of MLE-12 cells in response to overexpression of cathepsin D, and increased proliferation of fibroblasts when incubated with conditioned medium from cathepsin D–transfected cells. These observations fully corroborate our findings in HPS mice and human samples, in which highly increased levels of cathepsin D were observed in AECII, signifying its prominent role in the development of HPSIP. The development of AECII apoptosis and lung fibrosis in HPS1/2 mice was further strengthened by lipidomic profiling of lung tissue, particularly with a significant increase in glucosylceramides. In fibroblasts isolated from patients with Gaucher's disease, such an accumulation of GlcCer was found to cause oxidative stress and apoptosis (52). Moreover, accumulation of gangliosides (gangliosidosis) or sphingomyelin (Niemann-Pick disease) were shown to provoke the unfolded protein response, causing neuronal death (53, 54). In line with such reasoning, a severe ER stress response had been previously shown to be the primary cellular consequence of mutations of the *SFTPC* gene (55), a rare reason for development of familial forms of idiopathic interstitial pneumonias. Mutations in the BRICHOS domain of the carboxy-terminal part of pro–SP-C resulted in misfolding and accumulation of the proprotein, finally also leading to induction of ER stress and AECII apoptosis (55, 56). Furthermore, severe ER stress, with the induction of ATF4 and activation of the apoptosis mediator CHOP, was observed in HPSIP (both in mice and humans) in our study, similar to previous studies by our group in patients with sporadic IPF (57). This ER stress response in HPSIP could be due to increasing amounts of accumulating SP-B/C or retrograde stacking of lysosomal surfactant compounds into the ER. In any case, such additional ER stress adds further to the lysosomal stress–induced AECII apoptosis. Drawn against observations in IPF, these data suggest that apoptosis of alveolar epithelium due to chronic lysosomal/ER stress indeed represents a common observation in HPSIP (Figure 9) and a pivotal event in the evolution of lung fibrosis in general. ER stress has been implicated in many diseases such as Alzheimer's disease, diabetes, Parkinson disease, and, more recently, also in chronic obstructive pulmonary disease (58, 59). Increasing evidence suggests that certain chemical chaperons such as sodium 4-phenyl butyrate or butylated hydroxyanisole (which is also an antioxidant) may help to dampen the unfolded protein response, thereby preventing cells from undergoing ER stress–induced apoptosis (60, 61). As an attempt to rescue AECII from ER stress–induced cell death in HPSIP, use of similar agents may be discussed, but their ability to also circumvent lysosomal stress, the primary injurious event in HPSIP to AECII, has yet to be investigated.

Regarding the clinical similarities of IPF and HPSIP, it is an intriguing thought that the herein identified HPS1/2 mice would represent a much better model as compared with the widely used bleomycin model, in which excessive inflammation before the onset of lung fibrosis and its cessation after several weeks of bleomycin challenge are ascertained drawbacks. Lack of effective treatment for IPF or HPSIP makes HPS1/2 mice a more admissible murine fibrosis model.

Conflict of Interest Statement: P.M. does not have a financial relationship with a commercial entity that has an interest in the subject of this manuscript; M.K. does not have a financial relationship with a commercial entity that has an interest in the subject of this manuscript; I.H. does not have a financial relationship with a commercial entity that has an interest in the subject of this manuscript; G.L. does not have a financial relationship with a commercial entity that has an interest in the subject of this manuscript; G.S. does not have a financial relationship with a commercial entity that has an interest in the subject of this manuscript; B.R.C. holds $10,001–$50,000 in stock ownership or options in a health care sector mutual fund; P.M. does not have a financial relationship with a commercial entity that has an interest in the subject of this manuscript; S.B. does not have a financial relationship with a commercial entity that has an interest in the subject of this manuscript; W.S. does not have a financial relationship with a commercial entity that has an interest in the subject of this manuscript; C.R. received up to $1,000 from GlaxoSmithKline in consultancy fees; A.G. received $1,001–$5,000 from GlaxoSmithKline, $1,001–$5,000 from Actelion, $1,001–$5,000 from Activaero, and $10,001–$50,000 from Nycomed in advisory board fees, and $1,001–$5,000 from Actelion in lecture fees.

Acknowledgment: The authors thank Dr. Tim Weaver for helpful comments and criticism. The authors also thank Benjamin Loeh for technical assistance.

References

1. Hermansky F, Pudlak P. Albinism associated with hemorrhagic diathesis and unusual pigmented reticular cells in the bone marrow: report of two cases with histochemical studies. *Blood* 1959;14:162–169.
2. Li W, Rusiniak ME, Chintala S, Gautam R, Novak EK, Swank RT. Murine Hermansky-Pudlak syndrome genes: regulators of lysosome-related organelles. *Bioessays* 2004;26:616–628.
3. Huizing M, Gahl WA. Disorders of vesicles of lysosomal lineage: the Hermansky-Pudlak syndromes. *Curr Mol Med* 2002;2:451–467.
4. Anderson PD, Huizing M, Claassen DA, White J, Gahl WA. Hermansky-Pudlak syndrome type 4 (HPS-4): clinical and molecular characteristics. *Hum Genet* 2003;113:10–17.
5. Wei ML. Hermansky-Pudlak syndrome: a disease of protein trafficking and organelle function. *Pigment Cell Res* 2006;19:19–42.
6. Gahl WA, Brantly M, Troendle J, Avila NA, Padua A, Montalvo C, Cardona H, Calis KA, Gochuico B. Effect of pirfenidone on the

pulmonary fibrosis of Hermansky-Pudlak syndrome. *Mol Genet Metab* 2002;76:234–242.
7. Garay SM, Gardella JE, Fazzini EP, Goldring RM. Hermansky-Pudlak syndrome: pulmonary manifestations of a ceroid storage disorder. *Am J Med* 1979;66:737–747.
8. Harmon KR, Witkop CJ, White JG, King RA, Peterson M, Moore D, Tashijian J, Marinelli A, Bitterman PB. Pathogenesis of pulmonary fibrosis: platelet-derived growth factor precedes structural alterations in the Hermansky-Pudlak syndrome. *J Lab Clin Med* 1994;123:617–627.
9. Reynolds SP, Davies BH, Gibbs AR. Diffuse pulmonary fibrosis and HPS. *Thorax* 1994;49:617–618.
10. Nakatani Y, Nakamura N, Sano J, Inayama Y, Kawano N, Yamanaka S, Miyagi Y, Nagashima Y, Ohbayashi C, Mizushima M, *et al.* Interstitial pneumonia in Hermansky-Pudlak syndrome: significance of florid foamy swelling/degeneration (giant lamellar body degeneration) of type II pneumocytes. *Virchows Arch* 2002;437:304–313.
11. Pierson DM, Ionescu D, Qing G, Yonan AM, Parkinson K, Colby TC, Leslie K. Pulmonary fibrosis in Hermansky Pudlak syndrome: a case report. *Respiration* 2000;73:382–395.
12. Lyerla TA, Rusiniak ME, Borchers M, Jahreis G, Tan J, Ohtake P, Novak EK, Swank RT. Aberrant lung structure, composition, and function in a murine model of Hermansky-Pudlak syndrome. *Am J Physiol Lung Cell Mol Physiol* 2003;285:L643–L653.
13. Guttentag SH, Akhtar A, Tao JQ, Atochina E, Rusiniak ME, Swank RT, Bates SR. Defective surfactant secretion in a mouse model of Hermansky-Pudlak syndrome. *Am J Respir Cell Mol Biol* 2005;33:14–21.
14. Mahavadi P, Korfei M, Ruppert C, Seeger W, Guenther A. Evidence of surfactant accumulation and type II pneumocyte apoptosis in Hermansky-Pudlak syndrome [abstract]. *Am J Respir Crit Care Med* 2008;177:A823.
15. Mahavadi P, Korfei M, Markart P, Schmidt R, Seeger W, Guenther A, Ruppert C. Altered post-translational processing of pulmonary surfactant components in a murine model of Hermansky-Pudlak syndrome [abstract]. *Am J Respir Crit Care Med* 2006;3:A192.
16. Woessner JF. Determination of hydroxyproline in tissue and protein samples containing small proportions of this imino acid. *Arch Biochem Biophys* 1961;93:440.
17. Brasch F, Johnen G, Brasch AW, Guttentag SH, Schmiedl A, Kapp N, Suzuki Y, Müller KM, Richter J, Hawgood S, *et al.* Surfactant protein B in type II pneumocytes and intra-alveolar surfactant forms of human lungs. *Am J Respir Cell Mol Biol* 2004;30:449–458.
18. Brasch M, Brinke AT, Johnen G, Ochs M, Kapp N, Müller KM, Beers MF, Fehrenbach H, Richter J, Batenburg JJ, *et al.* Involvement of cathepsin H in the processing of the hydrophobic surfactant-associated protein C in type II pneumocytes. *Am J Respir Cell Mol Biol* 2002;26:659–670.
19. Ihrke G, Kyttala A, Russel MRG, Rous BA, Luzio JP. Differential use of two AP-3 mediated pathways by lysosomal membrane proteins. *Traffic* 2004;5:946–962.
20. Richmond B, Huizung M, Knapp J, Koshoffer A, Zhao Y, Gahl WA, Boissy RE. Melanocytes derived from patients with Hermansky-Pudlak syndrome types 1, 2 and 3 have distinct defects in cargo trafficking. *J Invest Dermatol* 2005;124:420–427.
21. Minarowska A, Miarowski L, Karwowska A, Gacko M. Regulatory role of cathepsin D in apoptosis. *Folia Histochem Cytobiol* 2007;45:159–163.
22. Kaedgal K, Johansson U, Oellinger K. The lysosomal protease cathepsin D mediates apoptosis induced by oxidative stress. *FASEB J* 2001;15:1592–1594.
23. Tang X, Yamanaka S, Miyagi Y, Nagashima Y, Nakatani Y. Lung pathology of pale ear mouse (model of Hermansky-Pudlak syndrome 1) and beige mouse (model of Chediak-Higashi syndrome): severity of giant lamellar body degeneration of type II pneumocytes correlates with interstitial inflammation. *Pathol Int* 2005;55:137–143.
24. Osanai K, Oikawa R, Higuchi J, Kobayashi M, Tsuchihara K, Iguchi M, Jongsu H, Toga H, Voelker DR. A mutation in Rab38 small GTPase causes abnormal lung surfactant homeostasis and aberrant alveolar structure in mice. *Am J Pathol* 2008;173:1265–1274.
25. Prueitt JL, Chi EY, Lagunoff D. Pulmonary surface-active materials in the Chediak-Higashi syndrome. *J Lipid Res* 1978;19:410–415.
26. McGarry MP, Reddington M, Novak EK, Swank RT. Survival and lung pathology of mouse models of Hermansky-Pudlak syndrome and Chediak-Higashi syndrome. *Proc Soc Exp Biol Med* 2003;220:162–168.
27. Young LR, Borchers MT, Allen HL, Gibbons RS, McCormack FX. Lung-restricted macrophage activation in the pearl mouse model of Hermansky-Pudlak syndrome. *J Immunol* 2006;176:4361–4368.
28. Raouhani FN, Brantly ML, Markello TC, Helip-Wooley A, O'Brien K, Hess R, Huizung M, Gahl WA, Gochuico BR. Alveolar macrophage dysregulation in Hermansky-Pudlak syndrome type 1. *Am J Respir Crit Care Med* 2009;180:1114–1121.
29. Glasser SW, Burhans MS, Korfhagen TR, Na CL, Sly PD, Ross GF, Ikegami M, Whitsett JA. Altered stability of pulmonary surfactant in SP-C–deficient mice. *Proc Natl Acad Sci USA* 2001;98:6366–6371.
30. Nogee LM. Alterations in SP-B and SP-C expression in neonatal lung disease. *Annu Rev Physiol* 2004;66:601–623.
31. Follonier L, Schaub S, Meister JJ, Hinz B. Myofibroblast communication is controlled by intercellular mechanical coupling. *J Cell Sci* 2008;121:3305–3316.
32. Guenther A, Schmidt R, Nix F, Yabut-Perez M, Guth C, Rosseau S, Siebert C, Grimminger F, Morr H, Velcovsky HG, *et al.* Surfactant abnormalities in idiopathic pulmonary fibrosis, hypersensitivity pneumonitis and sarcoidosis. *Eur Respir J* 1999;14:565–573.
33. Young LR, Pasula R, Gulleman PM, Deutsch GH, McCormack FX. Susceptibility of Hermansky-Pudlak mice to bleomycin-induced type II cell apoptosis and fibrosis. *Am J Respir Cell Mol Biol* 2007;37:67–74.
34. Suzuki T, Li W, Zhang Q, Karim A, Novak EK, Sviderskaya EV, Hill SP, Bennett DC, Levin AV, Nieuwenhuis HK, *et al.* Hermansky-Pudlak syndrome is caused by mutations in *HPS4*, the human homolog of the mouse light-ear gene. *Nat Genet* 2002;30:321–324.
35. Chiang PW, Oiso N, Gautam R, Suzuki T, Swank RT, Spritz RA. The Hermansky Pudlak syndrome 1 (HPS1) and HPS4 proteins are components of two complexes, BLOC 3 and BLOC 4. *J Biol Chem* 2003;278:20332–20337.
36. Nazarian R, Falcón-Pérez JM, Dell'Angelica EC. Biogenesis of lysosome-related organelles complex-3 (BLOC3): a complex containing the Hermansky-Pudlak syndrome (HPS) proteins, HPS1 and HPS4. *Proc Natl Acad Sci USA* 2003;100:8770–8775.
37. Falcón-Pérez JM, Nazarian R, Sabatti C, Dell'Angelica EC. Distribution and dynamics of Lamp1-containing endocytic organelles in fibroblasts deficient in BLOC-3. *J Cell Sci* 2005;118:5243–5255.
38. Dell'Angelica EC. The building BLOC(k)s of lysosomes and related organelles. *Curr Opin Cell Biol* 2004;16:458–464.
39. Kloer DP, Rojas R, Ivan V, Moriyama K. vanVlijmen T, Murthy N, Ghirlando R, van der Sluijs P, Hurley JH, Bonifacino JS. Assembly of the biogenesis of lysosome-related organelles complex-3 (BLOC-3) and its interaction with Rab9. *J Biol Chem* 2010;285:7794–7804.
40. Salazar G, Zlatic S, Craige B, Peden AA, Pohl J, Faundez V. Hermansky-Pudlak syndrome protein complexes associate with PI4 kinase type IIα in neuronal and nonneuronal cells. *J Biol Chem* 2009;284:1790–1802.
41. Newell-Litwa K, Chintala S, Jenkins S, Pare JF, McGha L, Smith Y, Faundez V. Hermansky-Pudlak protein complexes, AP-3 and BLOC-1, differentially regulate presynaptic composition in the striatum and hippocampus. *J Neurosci* 2010;30:820–831.
42. Litwa KN, Seong E, Burmeister M, Faundez V. Neuronal and non-neuronal functions of the AP-3 sorting machinery. *J Cell Sci* 2007;120:531–541.
43. Harrison-Lavoie KJ, Michaux G, Hewlett L, Kaur J, Hannah MJ, Lui-Roberts WW, Norman KE, Cutler DF. P-selectin and CD63 use different mechanisms for delivery to Weibel-Palade bodies. *Traffic* 2006;7:647–662.
44. Dell'Angelica EC, Shotelersuk V, Aguilar RC, Gahl WA, Bonifacino JS. Altered trafficking of lysosomal proteins in Hermansky-Pudlak syndrome due to mutations in β3A subunit of AP-3 adaptor. *Mol Cell* 1999;3:11–21.
45. Dell'Angelica EC, Augilar RC, Wolins N, Hazelwood S, Gahl WA, Bonifacino JS. Molecular characterization of the protein encoded by the Hermansky-Pudlak syndrome type 1 gene. *J Biol Chem* 2000;275:1300–1306.
46. Feng L, Novak EK, Hartnell LM, Bonifacino JS, Collinson LM, Swank RT. The Hermansky-Pudlak syndrome 1 (HPS1) and HPS2 genes independently contribute to the production and function of platelet dense granules. *Blood* 2002;99:1651–1658.
47. Kristova V, Canova R. Pulmonary surfactant: properties, relation to the respiratory distress syndrome in neonates and possibilities of its prevention and therapy. *Bratisl Lek Listy (Tlacene Vyd)* 1992;93:41–49.
48. Olkkonen VM, Ikonen E. When intracellular logistics fails: genetic defects in membrane trafficking. *J Cell Sci* 2006;119:5031–5045.
49. Baumgartner HK, Gerasimenko JV, Thorne C, Ashurst LH, Barrow SL, Chvanov MA, Gillies S, Criddle DN, Tepikin AV, Petersen OH, *et al.* Caspase-8–mediated apoptosis induced by oxidative stress is inde-

pendent of the intrinsic pathway and dependent on cathepsins. *Am J Physiol* 2007;293:G296.
50. Blomgran R, Zheng L, Stendahl O. Cathepsin-cleaved Bid promotes apoptosis in human neutrophils via oxidative stress–induced lysosomal membrane permeabilization. *J Leukoc Biol* 2007;81:1213–1223.
51. Li X, Rayford H, Shu R, Zhuang J, Uhal BD. Essential role for cathepsin D in bleomycin-induced apoptosis of alveolar epithelial cells. *Am J Physiol Lung Cell Mol Physiol* 2004;287:L46–L51.
52. Deganuto M, Pittis MG, Pines A, Dominissini S, Kelley MR, Garcia R, Quadrifoglio F, Bembi B, Tell G. Altered intracellular redox status in Gaucher disease fibroblasts and impairment of adaptive response against oxidative stress. *J Cell Physiol* 2007;212:223–235.
53. Kolter T, Sandhoff K. Sphingolipid metabolism diseases. *Biochim Biophys Acta* 2006;1758:2057–2079.
54. Tessitore A, Martin MD, Sano R, Ma Y, Mann L, Ingrassia A, Laywell ED, Steindler DA, Hendershot LM, d'Azzo A.G_{M1}-ganglioside–mediated activation of the unfolded protein response causes neuronal death in a neurodegenerative gangliosidosis. *Mol Cell* 2004;15:753–766.
55. Mulugeta S, Nguyen V, Russo SJ, Muniswamy M, Beers MF. A surfactant protein C precursor protein BRICHOS domain mutation causes endoplasmic reticulum stress, proteasome dysfunction, and caspase 3 activation. *Am J Respir Cell Mol Biol* 2005;32:521–530.
56. Wang WJ, Mulugeta S, Russo SJ, Beers MF. Deletion of exon 4 from human surfactant protein C results in aggresome formation and generation of a dominant negative. *J Cell Sci* 2003;116:683–692.
57. Korfei M, Ruppert C, Mahavadi P, Henneke I, Markart P, Koch M, Lang G, Fink L, Bohle RM, Seeger W, *et al.* Epithelial endoplasmic reticulum stress and apoptosis in sporadic idiopathic pulmonary fibrosis. *Am J Respir Crit Care Med* 2008;178:838–846.
58. Yoshida H. ER stress and diseases. *FEBS J* 2007;274:630–658.
59. Malhotra D, Thimmulappa R, Vij N, Navas-Acien A, Sussan T, Merali S, Zhang L, Kelsen SG, Myers A, Wise R, *et al.* Heightened endoplasmic reticulum stress in the lungs of patients with chronic obstructive pulmonary disease: the role of Nrf2-regulated proteasomal activity. *Am J Respir Crit Care Med* 2009;180:1196–1209.
60. Yam GH, Gaplovska-Kysela K, Zuber C, Roth J. Sodium 4-phenylbutyrate acts as a chemical chaperone on misfolded myocillin to rescue cells from endoplasmic reticulum stress and apoptosis. *Invest Ophthalmol Vis Sci* 2007;48:1683–1690.
61. Malhotra JD, Miao H, Zhang K, Wolfson A, Pennathur S, Pipe SW, Kaufman RJ. Antioxidants reduce endoplasmic reticulum stress and improve protein secretion. *Proc Natl Acad Sci USA* 2008;105:18525–18530.